ELSEVIER

Catalysis Today 56 (2000) 265–273

CATALYSIS TODAY

www.elsevier.com/locate/cattod

Permeation characteristics of butane isomers through MFI-type zeolitic membranes

Takaaki Matsufuji [a], Norikazu Nishiyama [a], Korekazu Ueyama [a], Masahiko Matsukata [b,*]

[a] *Division of Chemical Engineering, Graduate School of Engineering Science, Osaka University, 1-3 Machikaneyama-cho, Toyonaka-shi, Osaka 560-8531, Japan*

[b] *Department of Applied Chemistry, Waseda University, 3-4-1 Okubo, Shinnjyuku-ku, Tokyo 169-8555, Japan*

Abstract

MFI-type◆ zeolitic membranes were prepared by a vapor-phase transport method on porous α-alumina flat disks. Pure or mixed gas permeation measurements of butane isomers were performed at 375 K using two methods: pressure gradient (PG) and concentration gradient (CG) methods. Pure gas permeation measurements of H_2, He, CH_4, N_2, O_2, CO_2 and SF_6 were also carried out using PG method. Counter-diffusion of helium as a sweep gas was evaluated by determining the gas composition at the outlet of the feed side. It was confirmed that the counter-diffusion of helium occurs only when the total pressure of the feed side was <80 kPa.

In the mixed gas permeation measurements, the value of separation factor depended on the method of gas permeation. The separation factors of *n*-butane to *i*-butane were ca. 10 in the PG method and 30–60 in the CG method.

Keywords: Butane isomers; Zeolitic membranes; Pressure gradient; Concentration gradient

1. Introduction

In this decade, much attention has been paid to zeolitic membranes for gas separation, pervaporation and membrane catalysis [1–22]. Zeolitic membranes can be useful for separating mixtures of isomer with similar boiling points but different molecular sizes. Most of the zeolitic membranes reported in the literature are MFI-type zeolitic membranes synthesized by a hydrothermal technique, which is conventional for the preparation of granular zeolites.

Zeolite has been known to be a catalyst for catalytic cracking. Zeolitic membrane also possesses catalytic activity, either acid activity, or metal activity, or both. The catalytic activity can be modified according to the needs of the reaction involved [1]. For example, the acid activity of siliceous zeolites can be adjusted by the amount of trivalent elements (especially aluminum). Substitution by a trivalent element such as aluminum introduces a negative charge. The charge is to be balanced by cation exchange with proton and alkaline earth metal cations.

Suzuki [2] presented a large number of examples of membrane catalysis with ultrathin zeolitic membranes. He added reactants to one side of the zeolitic membrane and removed products from the other side. A good example of the zeolitic membrane reactor is for a feed of hydrogen/propene/*i*-butane mixture over a Pt–Ca A-type zeolitic membrane. Only hydrogen and propane appeared on the permeate side, indicating that hydrogenation and separation simultaneously

* Corresponding author. Tel./fax: +81-3-5286-3850.
E-mail address: mmatsu@mn.waseda.ac.jp (M. Matsukata).

0920-5861/00/$ – see front matter
PII: S0920-5861(99)00284-9

Table 1
Results of the separation of butane isomers with MFI-type zeolitic membrane

Support	Permeation method method	Temperature (K)	Ideal selectivity (–) *n*-/*i*-butane	Separation factor (–) *n*-/*i*-butane	Reference
Stainless steel/disk	CG	298	ca. 50	–	[3]
γ-Alumina/tube	PG, CG	298	22	–	[4]
		443	0.6	–	
α-Alumina/disk	PG	303	18.4	–	[5,6]
		458	33.1	–	
α-Alumina/disk	CG	298	90	52	[7]
		473	11	11	
Stainless steel/disk	CG	295	58	27	[8]
		403	–	23	
α-Almunia/disk	CG	373	1.5–12	18–26	[9]
γ-Alumina/tube	PG	300	14 (γ-Alumina)	33 (365 K)	[11]
α-Alumina/tube	PG	461	4.8 (α-Alumina)	18 (383 K)	

occurred. They did not report the information on numerical values of fluxes or stabilities of the membranes. These results would significantly expand the potential application of membrane catalysis using zeolite.

The quality of the membrane is important for the application of zeolitic membranes in industrial processes. Many research groups reported the pure and mixed gas permeation measurements of butane isomers, as listed in Table 1. *n*-Butane/*i*-butane permselectivity shows good indication of the quality of MFI-type zeolitic membrane. For single or mixed gas permeation measurements of butane isomers, two types of measurements have generally been performed: pressure gradient (PG) and concentration gradient (CG) methods.

In the PG method, the flux is determined at a given PG. On the other hand, the total pressure on both sides of membrane is generally kept at atmospheric pressure in the CG method. Helium or argon was generally used as a sweep gas in the gas permeation measurements. These sweep gases seemed to diffuse to the feed side during permeation measurements. To evaluate the permeation measurements, van de Graaf et al. [13] compared the data obtained from both PG and Wicke–Kallenbach methods. They claimed that the sweep gas significantly influenced permeation and such effect depended on the nature of sweep gas and on the magnitude of its counter permeation. It is difficult to conclude that previous permeation data were free from the effect of the counter-diffusion of sweep gas.

In this study, MFI-type zeolitic membranes were prepared by vapor-phase transport (VPT) method [23–30]. Both single gas permeation measurements and mixed gas separations were carried out to evaluate the influence of the method used for permeation measurement of butane isomers (pressure or concentration gradient) on the selectivity and on the counter-diffusion of the sweep gas with compact and less compact MFI-type zeolitic membrane.

2. Experimental

2.1. Preparation of parent gel

A parent aluminosilicate sol with SiO_2/Al_2O_3 ratio of 1000 was prepared using colloidal silica containing 30 wt.% of SiO_2, 0.5 wt.% of Al_2O_3 and 0.4 wt.% of Na_2O (Nissan Chemical Co., Ltd.). First, colloidal silica was mixed with NaOH(4N) at 303 K. A flat porous α-alumina support (Nihon Gaishi Co., Ltd.) with a cross-sectional area of $1.0 \times 10^{-4}\,m^2$ and an average pore diameter of 0.1 μm was dipped into the parent sol at 303 K for 1 day. Then the sol was forced to penetrate into the pores of alumina support by evacuating the support from one side for 1 h, as shown in Fig. 1. As a pretreatment of an alumina support, the support was treated with colloidal silica at the pH of about 10 to depress the dissolution of alumina during membrane synthesis.

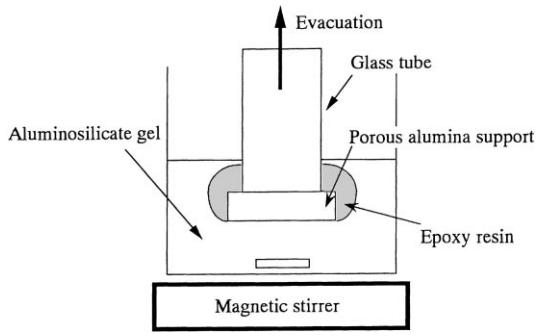

Fig. 1. Schematic diagram of experimental apparatus for coating α-alumina support with aluminosilicate sol.

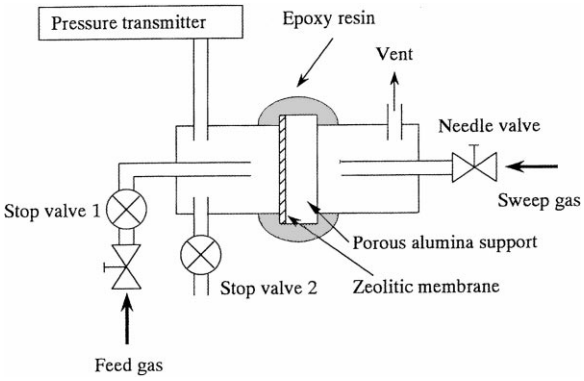

Fig. 2. Schematic diagram of experimental apparatus for permeation measurements.

2.2. Crystallization of dry gel by vapor-phase transport method

Crystallization was carried out in an autoclave. A mixture of ethylenediamine (EDA), triethylamine (Et_3N) and water (EDA: 2.0 Et_3N: H_2O, volume ratio) was poured in the bottom to produce vapor. The support coated with the parent gel was horizontally set on the partition in the middle of the autoclave. Crystallization was performed in gaseous environment at 453 K for 72 h at autogenous pressure. As-synthesized MFI membranes were calcined in air at 773 K for 10 h. The heating rate of 0.05–0.1 K min^{-1} was adopted in the temperature range from 473 to 773 K. The weight gain of alumina support during gel coating, crystallization and calcination was ca. 100 mg. The crystallinity and structure of the products were analyzed by X-ray diffraction (XRD) with Cu Kα radiation (Philips X's Pert-MRD). The morphology of products was examined by scanning electron microscopy (SEM) (Hitachi S-2250).

2.3. Evaluation of the compactness of zeolitic membranes

For evaluating compactness of MFI membranes, the pervaporation of 1,3,5-triisopropylbenzene (TIPB), which has a kinetic diameter (0.85 nm) larger than the pore dimensions of MFI (0.53×0.56, 0.51×0.55 nm), was carried out for 10 h at 295 K. A zeolitic membrane with a cross-sectional area of 0.50×10^{-4} m^2 was attached on an end of a glass tube, and placed in liquid TIPB. The permeation side was kept under vacuum. The permeant was collected for 10 h in a cold trap using liquid nitrogen and analyzed by a gas chromatograph with a flame ionization detector.

2.4. Gas permeation measurements

2.4.1. Pure gas permeation measurement

The pure gas permeation tests for H_2, He, CH_4, N_2, O_2, CO_2, *n*-butane, *i*-butane and SF_6 were performed using the PG method at 375 K. Fig. 2 shows the schematic diagram of experimental apparatus for determining the permeance. Epoxy resin was used as a seal material between a glass tube with a membrane and an apparatus. As a pretreatment for a gas permeation test, water adsorbed in the zeolitic membrane was removed by evacuating at 420 K for 2 h. The heating rate of 0.5–1.0 K min^{-1} was adopted. The total pressure of feed side was measured using the pressure transmitter. Helium was used as a sweep gas in the permeate side at atmospheric pressure. The permeance of H_2, He, CH_4, N_2, O_2, CO_2, *n*-butane, *i*-butane and SF_6 through an MFI membrane at 160 kPa was determined by using the rate of pressure reduction of the feed side from 165 to 155 kPa. They were calculated by using Eqs. (1) and (2):

$$\frac{\partial n}{\partial t} = \frac{\partial p}{\partial t} \times \frac{V}{RT} \tag{1}$$

$$\text{Permeance (mol m}^{-2}\,\text{s}^{-1}\,\text{Pa}^{-1}) = \frac{\partial n}{\partial t} \times \frac{1}{A\Delta p} \tag{2}$$

where *n* represents the amount of permeant (mol), *t*, time (s), *p*, pressure on the feed side (Pa), *V*, dead

volume on the feed side (7.0 cm^3), R, gas constant (8.314 $J\,mol^{-1}\,K^{-1}$), T, temperature (K), A, effective membrane area ($0.50 \times 10^{-4}\ m^2$) and Δp, partial pressure difference between the feed and permeant sides (Pa).

2.4.2. Evaluation of counter-diffusion of helium

The total pressure of feed side was kept at 180 kPa by feeding pure *n*-butane, after the pretreatment. After 24 h, feeding of *n*-butane was stopped by closing stop valve 2 shown in Fig. 2. The measurement was started after the total pressure of feed side was decreased to 160 kPa. Helium was used as a sweep gas and the pressure of permeate side was kept at atmospheric pressure throughout the permeation measurements. The feed gas was analyzed for the mole fraction of gas in the feed side by a gas chromatograph (Ohkura, Model 802) with a TC detector and a packed column (Porapak Type Q, 2 m × 1/8 in. (3.2 mm)). Similar procedure was used for measuring *i*-butane permeation, whereas only the total pressure of feed side was measured.

2.4.3. Mixed gas permeation measurement

In the PG method, the total pressure difference between the feed and permeation sides was kept at 60 kPa, while both sides of the membrane were kept at atmospheric pressure in the CG method, as shown in Fig. 3. Helium was used as a sweep gas. In the CG method, the total feed rates of butane isomers were 50–60 $cm^3\,min^{-1}$. The permeate and retentate gas were analyzed by gas chromatograph. Ideal selectivity was calculated from the flux ratio of *n*-butane to *i*-butane. Separation factor was calculated from the following equation,

$$\text{Separation factor} = \frac{(X_n/X_i)\ \text{permeate}}{(X_n/X_i)\ \text{feed}} \quad (3)$$

where X_n and X_i represent mole fractions of *n*-butane (%) and *i*-butane (%), respectively.

3. Results and discussion

3.1. Compactness of MFI-type zeolitic membrane

Almost half synthesized membranes were gas-tight (flux of helium $< 1.0 \times 10^{-8}\ mol\,m^{-2}\,s^{-1}$) after synthesis. When crystallization was not complete, a small amount of helium permeation was observed. The quality of the membranes after calcination was tested by the pervaporation of TIPB. After calcination, we obtained three polycrystalline MFI-type zeolitic membranes (membranes A, B and C) which were gas-tight before calcination.

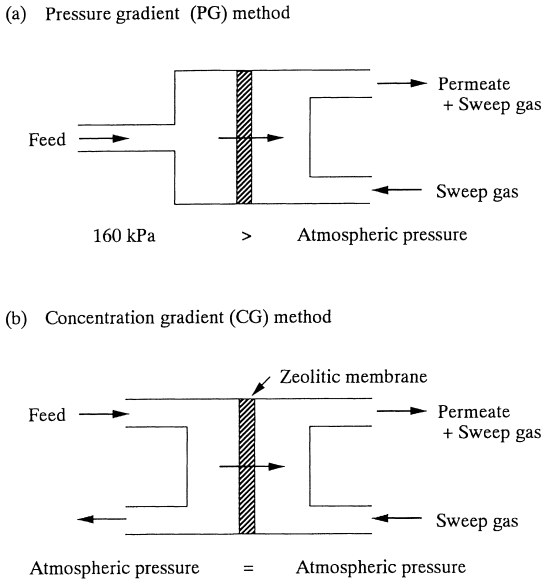

Fig. 3. Schematic diagram of gas permeation measurements.

Table 2 shows the flux of TIPB through the MFI membranes. After the pervaporation test, no permeation of TIPB through membrane A was detected, indicating that the flux of TIPB was less than $1.0 \times 10^{-9}\ mol\,m^{-2}\,s^{-1}$, the detection limit in this experiment. Therefore, it was concluded that membrane A was practically pinhole-free. On the other hand, the permeation fluxes of TIPB were 3.0×10^{-7} and $1.2 \times 10^{-6}\ mol\,m^{-2}\,s^{-1}$ for membrane B and C, respectively. Membranes B and C have pinholes larger than TIPB molecule.

Fig. 4 shows the SEM images of top and cross-sectional views of membrane A. On membrane

Table 2
Flux of TIPB through the MFI membranes

	Flux of TIPB ($mol\,m^{-2}\,s^{-1}$)
Membrane A	$<1.0 \times 10^{-9}$
Membrane B	3.0×10^{-7}
Membrane C	1.2×10^{-6}

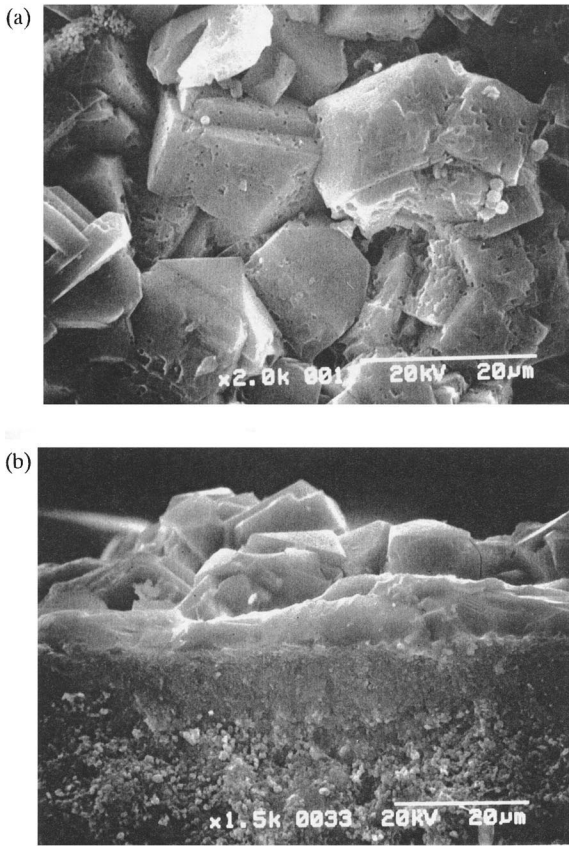

Fig. 4. SEM images for the (a) top view and (b) cross-sectional view of membrane A.

A, a top layer formed on the alumina support was ca. 20 μm thick and MFI zeolite was also formed in the interior of support was also ca. 20 μm thick.

3.2. Pure gas permeation measurement

Fig. 5 shows the permeances of H_2, He, CH_4, N_2, O_2, CO_2, *n*-butane, *i*-butane and SF_6 through membrane A as a function of kinetic diameter of molecule at 375 K. Molecules such as CO_2 and *n*-butane smaller than the channels of an MFI (0.53×0.56, 0.51×0.55 nm) showed greater permeances. On the other hand, the permeance of *i*-butane (0.50 nm) and SF_6 (0.55 nm), whose sizes are comparable to the size of the channels of MFI, were very low. The permeance ratios of *n*-butane/*i*-butane and *n*-butane/SF_6 were 60 and 385, respectively.

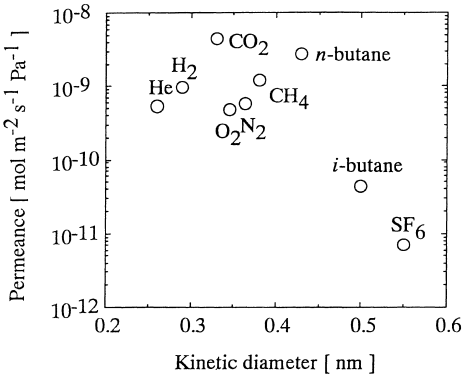

Fig. 5. Permeances as a function of kinetic diameter. Temperature: 375 K; partial pressure difference: 160 kPa.

3.3. Evaluation of counter-diffusion of helium

Counter-diffusion of the inert sweep gas can usually affect the permeation of feed components. The evaluation of counter-diffusion of the sweep gas is essential to understand the inherent permeances of feed components.

Fig. 6 shows the time course of the total pressure of feed side and the mole fraction of *n*-butane on the feed side for membrane A. It is worth noting that the total pressure of feed side had a minimum with time course and its value of 44.0 kPa was less than atmospheric pressure for the *n*-butane permeation test with membrane A. As shown in Fig. 6, the counter-diffusion of helium occurs only when the total pressure of the feed side was <80 kPa. Namely, *n*-butane dominantly permeated through membrane A from the feed side to the permeate one, and helium was difficult to enter the micropores of MFI crystals, even under the conditions that the total pressure of feed side was less than that of permeate side. When the total pressure of feed side was above 80 kPa, thus, the permeation data seemed to be free from the effect of the counter-diffusion of sweep gas. In the permeation measurement of *i*-butane with membrane A (not shown), the total pressure of feed side also had a minimum at 80.0 kPa.

On the other hand, in the permeation test with membrane B, the mole fraction of *n*-butane on the feed side started to decrease even when the total pressure of the feed side was higher than atmospheric pressure, as shown in Fig. 7. For membrane C, only the

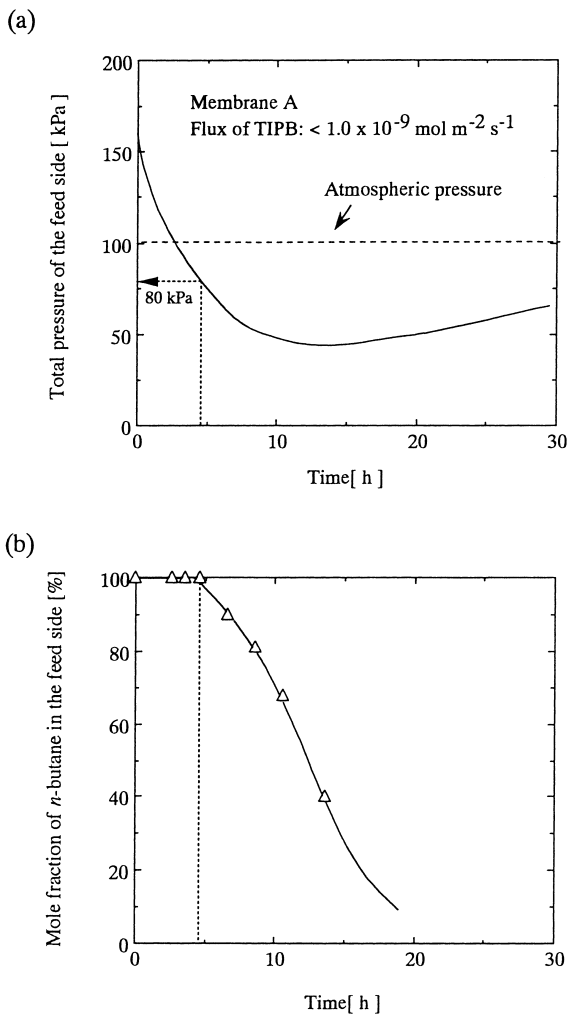

Fig. 6. Time course of (a) the total pressure of feed side and (b) the mole fraction of *n*-butane in the feed side with membrane A. Temperature: 375 K.

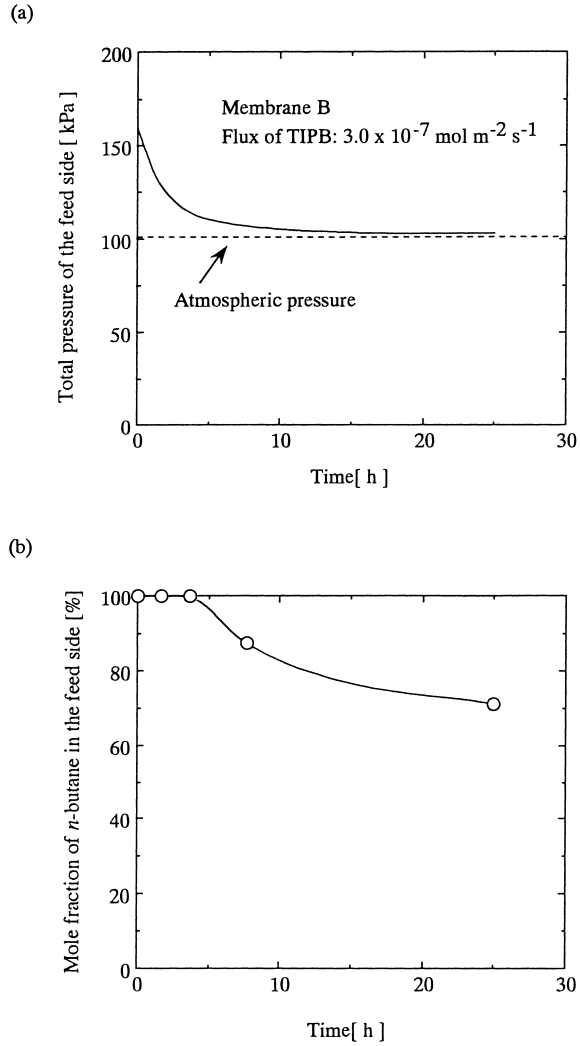

Fig. 7. Time course of (a) the total pressure of feed side and (b) the mole fraction of *n*-butane in the feed side with membrane B. Temperature: 375 K.

pressure change of the feed side was measured, and it quickly and monotonously approached to atmospheric pressure.

The compactness of MFI membrane would be essential to explain these permeation behavior. *n*-Butane molecules adsorbed might have filled the micropores of MFI crystals. Such pore filling would particularly be apparent with a compact membrane at lower temperatures. Even if the total pressure of feed side was lower than atmospheric pressure, the effect of pore filling possibly would still dominate the permeation behavior. *n*-Butane molecules filling the micropores of MFI crystals may inhibit the entrance of helium into the micropores of MFI.

On the other hand, *n*-butane seemed to permeate through pinholes in membrane B rather than the micropores of MFI crystals. *n*-Butane and helium can pass through each other in the pinholes of membrane B.

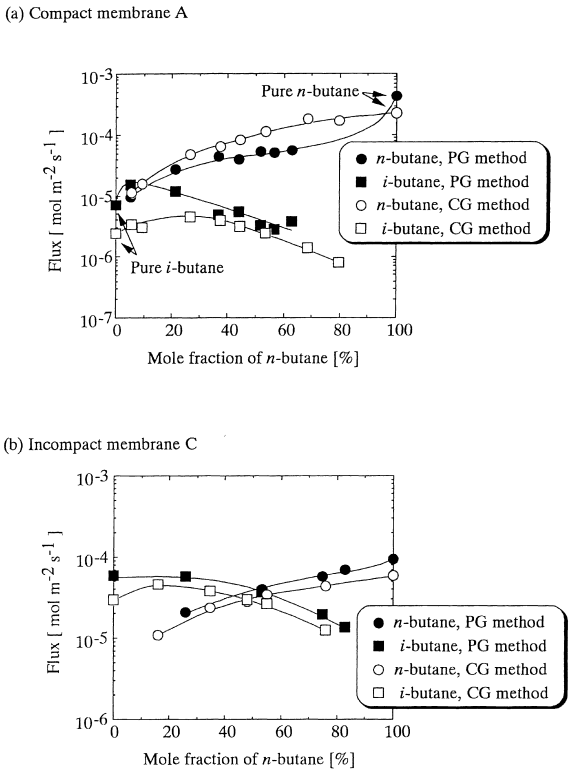

Fig. 8. Fluxes of butane isomers through MFI membranes as a function of mole fraction of *n*-butane in the feed. Temperature: 375 K; closed key: PG method; open key: CG method.

3.4. *n*-Butane/*i*-butane mixed gas separations

The permeation behaviors of *n*-butane and *i*-butane were studied with two types of gas permeation measurements at 375 K; PG and CG methods. It is not necessary to consider the effects of the counter-diffusion of helium with membrane A, because the total pressure of feed side was always above 80 kPa in these experimental procedure. Fig. 8 shows the fluxes of butane isomers through compact membrane A and incompact membrane C as a function of the mole fraction of *n*-butane in the feed.

In both permeation measurements using the PG and CG methods with membrane A, the flux of *n*-butane increased with increasing mole fraction of *n*-butane in the feed. It should be noted that the flux of *i*-butane had a maximum at around 25% of the mole fraction of *n*-butane in the CG method and 10% in the PG method, respectively. These results reveal that the permeation of *i*-butane was enhanced in the binary mixture. The results shown in Fig. 8 for the binary mixture show unique trend. *i*-Butane molecules might squeeze into the pore, accompanied by *n*-butane molecules. In the CG method, the flux of *n*-butane is higher than the flux of *i*-butane at low *n*-butane concentration for the membrane A. We suppose that a preferential distribution of *n*-butane and *i*-butane in the zeolite channels strongly depends on the concentration of the butane isomers on the feed side.

On the other hand, this is not true for the membrane C. Butane isomers seemed to permeate through pinholes in membrane C rather than the micropores of MFI crystals.

The PG method, where 60 kPa of total pressure difference was employed, gave a higher flux of *i*-butane and a lower flux of *n*-butane using membrane A, compared with those for the CG method. *i*-Butane molecules, adsorbed in the micropores of MFI, seem to reduce the diffusion and permeability of *n*-butane. On the other hand, the fluxes of both *n*-butane and *i*-butane in the PG method with membrane C were greater than those in the CG method.

Takaba et al. [31] presented the MD simulation of the mixed gas separation of butane isomers at 373 K. They reported that the permeation *n*-butane was observed, whereas *i*-butane did not permeate. However the diffusion of both isomers into the zeolite pores was observed. They concluded that the few diffused *i*-butane molecules reduced the diffusion and permeability of *n*-butane. The kinetic diameter of *i*-butane (0.50 nm) is larger than that of *n*-butane (0.43 nm). The micropores of MFI crystals are so narrow that *n*-butane and *i*-butane cannot pass through each other, possibly except at an intersection. The diffusion in such a narrow pore seems to be controlled by a molecule with a smaller permeation rate, i.e., *i*-butane molecule.

Fig. 9 shows the separation factor of butane isomer mixture through compact membrane A and incompact membrane C as a function of the mole fraction of *n*-butane in the feed. In the unary gas system, the ideal selectivity of *n*-butane to *i*-butane for membrane A was 60 in the PG method and 95 in the CG method. For binary mixtures, the separation factor also depended on the method of gas permeation: that of *n*-butane to *i*-butane was ca. 10 in the PG method and 30–60 in the CG method.

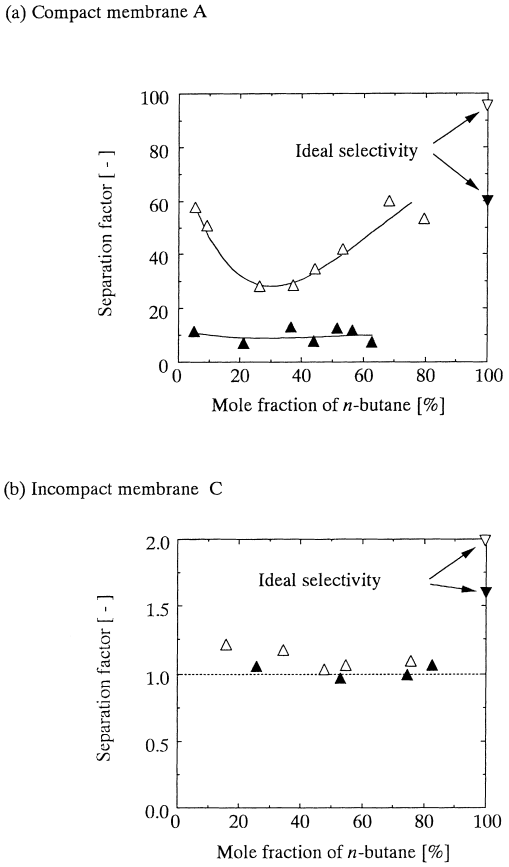

Fig. 9. Separation factor of butane isomers as a function of mole fraction of *n*-butane in the feed. Temperature: 375 K; closed key: PG method; open key: CG method.

On the other hand, the ideal selectivity of *n*-butane to *i*-butane using membrane C was only 1.6 in the PG method and 2.0 in the CG method. For the binary mixtures, the separation factors of *n*-butane to *i*-butane were ca. 1.0 in the PG method and 1.1 in the CG method, which are 1/30–1/60 of those for membrane A. These lead to a conclusion that the compactness of MFI membrane is essential to separate butane isomer mixtures at 375 K.

4. Conclusions

Polycrystalline MFI-type zeolitic membranes have been prepared by using vapor-phase transport method. In the permeation measurements, the compactness of MFI membrane is essential to obtain data, which are intrinsic to discuss the permeation through zeolitic layer. Using compact membrane, the permeation data free from the effects of counter-diffusion of helium were obtained by both PG method and CG method were free from the effects of counter-diffusion of helium. On the other hand, inert sweep gas permeated through pinholes of incompact membranes.

In the unary system using a compact membrane, small molecules such as CO_2 and *n*-butane showed greater permeances than those for large molecules, such as *i*-butane and SF_6. The permeance ratios of *n*-butane/*i*-butane and *n*-butane/SF_6 were 60 and 385, respectively.

In the binary system, the flux of *i*-butane had a maximum at around 25% of mole fraction of *n*-butane in the CG method and 10% in the PG method, respectively. This result reveals that permeation of *i*-butane was encouraged in the binary system.

The PG method gave a higher flux of *i*-butane and a lower flux of *n*-butane, compared with those for the CG method. *i*-Butane molecules may fill the micropore of MFI crystals and block their pore mouth. For binary mixtures, the separation factor depends on the method of gas permeation. The separation factors of *n*-butane to *i*-butane were ca. 10 in the PG method and 30–60 in the CG method at 375 K.

Acknowledgements

The authors are grateful to NGK Insulators, Ltd. for supplying α-alumina supports, and the authors thank GHAS laboratory at Osaka University form the SEM measurements.

References

[1] J.L. Falconer, R.D. Noble, D.P. Sperry, in: R.D. Noble, S.A., Stern (Eds.), Membrane Separations Technology. Principles and Applications, Elsevier, Amsterdam, 1995 (Chapter 14).
[2] H. Suzuki, US patent 4699892, 1987.
[3] E.R. Geus, H. Bekkum, W.J.W. Bakker, J.A. Moulijin, Microporous Mater. 1 (1993) 131–147.
[4] C. Bai, M.-D. Jia, J.L. Falconer, R.D. Noble, J. Membr. Sci. 105 (1995) 79–87.
[5] Y. Yan, M. Tsapatsis, G.R. Gavalas, M.E. Davis, J. Chem. Soc., Chem. Commun. (1995) 227–228.

[6] Y. Yan, M.E. Davis, G.R. Gavalas, Ind. Eng. Chem. Res. 34 (1995) 1652–1661.
[7] Z.A.E.P. Vroon, K. Keizer, M.J. Gilde, H. Verweij, A.J. Burggraaf, J. Membr. Sci. 113 (1996) 293–300.
[8] W.J.W. Bakker, F. Kapteijn, J. Poppe, J.A. Moulijn, J. Membr. Sci. 117 (1996) 57–78.
[9] K. Kusakabe, S. Yoneshige, A. Murata, S. Morooka, J. Membr. Sci. 116 (1996) 39–46.
[10] K. Kusakabe, A. Murata, T. Kuroda, S. Morooka, J. Chem. Eng. Jpn. 30 (1997) 72–78.
[11] J. Coronas, J.L. Falconer, R.D. Noble, AIChE J. 43 (1997) 1797–1812.
[12] R.D. Noble, J.L. Falconer, Catal. Today 25 (1995) 209–212.
[13] J.M. van de Graaf, F. Kapteijn, J.A. Moulijn, J. Membr. Sci. 144 (1998) 87–104.
[14] F. Kapteijn, W.J.W. Bakker, J. van de Graaf, G. Zheng, J. Poppe, J.A. Moulijn, Catal. Today 25 (1995) 213–218.
[15] T. Sano, M. Hasegawa, Y. Kawakami, Y. Kiyozumi, H. Yanagishita, D. Kitamoto, F. Mizukami, Stud. Surf. Sci. Catal. 84 (1994) 1175–1182.
[16] M.J. den Exter, J.C. Jansen, J.M. van de Graaf, F. Kapteijn, H. van Bekkum, Stud. Surf. Sci. Catal. 102 (1996) 413–454.
[17] H. Kita, Maku (Membrane) 20 (1995) 169–182.
[18] Q. Liu, R.D. Noble, J.L. Falconer, H.H. Funke, J. Membr. Sci. 117 (1996) 163–174.
[19] C.D. Baertsch, H.H. Junke, J.L. Falconer, R.D. Noble, J. Phys. Chem. 100 (1996) 7676–7679.
[20] H. Funke, A.M. Argo, C.D. Baertsch, J.L. Falconer, R.D. Noble, J. Chem. Soc., Faraday Trans. 92 (1996) 2499–2502.
[21] J.F. Smetana, J.L. Falconer, R.D. Noble, J. Membr. Sci. 114 (1996) 127–130.
[22] E. Lewis John Jr., G.R. Gavalas, M.E. Davis, AIChE J. 43 (1997) 83–90.
[23] W. Xu, J. Dong, Jinping Li, Jianquan Li, F. Wu, J. Chem. Soc., Chem. Commun. (1990) 755–756.
[24] M.H. Kim, H.X. Li, M.E. Davis, Microporous Mater. 1 (1993) 191–200.
[25] M. Matsukata, N. Nishiyama, K. Ueyama, Microporous Mater. 1 (1993) 219–222.
[26] M. Matsukata, N. Nishiyama, K. Ueyama, Microporous Mater. 7 (1996) 109–117.
[27] N. Nishiyama, K. Ueyama, M. Matsukata, Microporous Mater. 7 (1996) 299–308.
[28] N. Nishiyama, T. Matsufuji, K. Ueyama, M. Matsukata, Microporous Mater. 12 (1997) 293–303.
[29] E. Kikuchi, K. Yamashita, S. Hiromoto, K. Ueyama, M. Matsukata, Microporous Mater. 11 (1997) 107–116.
[30] N. Nishiyama, Synthesis of zeolitic membranes by vapor-phase transport method and their separation properties, Ph.D. Thesis, 1997.
[31] H. Takaba, R. Koshita, K. Mizukami, Y. Oumi, N. Ito, M. Kubo, A. Miyamoto, J. Membr. Sci. 134 (1997) 127–139.